PROCEEDINGS OF SPIE

SPIEDigitalLibrary.org/conference-proceedings-of-spie

The radiation environment at L2 as seen by Gaia

Ralf Kohley
Cian M. Crowley
Philippe Garé
François Chassat
Alexander D. Short
Juan M. Martin-Fleitas
Alcione Mora
Asier Abreu-Aramburu
Thibaut Prod'homme

SPIE.

The radiation environment at L2 as seen by Gaia

Ralf Kohley*[a], Cian M. Crowley[ab], Philippe Garé[c], François Chassat[d], Alexander D. Short[c], Juan M. Martin-Fleitas[ae], Alcione Mora[ae], Asier Abreu-Aramburu[af], Thibaut Prod'homme[c]

[a]European Space Agency, European Space Astronomy Centre (ESAC), P.O. Box 78, 28691 Villanueva de la Cañada (Madrid), Spain;
[b]HE Space Operations BV, Huygensstraat 44, 2201 DK Noordwijk, The Netherlands;
[c]European Space Agency, European Space Research and Technology Centre (ESTEC), P.O. Box 299, 2200 AG, Noordwijk, the Netherlands;
[d]Airbus Defense and Space, 31 Rue des Cosmonautes, 31402 Toulouse Cedex 4, France;
[e]Aurora Technology, Crown Business Centre, Heereweg 345, 2161 CA Lisse, The Netherlands;
[f]Elecnor Deimos Space, Ronda de Poniente 19, Edicación Fiteni VI, 28760 Tres Cantos, Madrid, Spain;

ABSTRACT

The radiation environment at L2 is of great importance to the science instruments of Gaia. Especially the non-ionising damage to the CCDs and the resulting increase in charge transfer inefficiency will ultimately limit the achievable science performance. With its launch in December 2013 for a nominal mission of 5 years Gaia is continuously collecting invaluable information of radiation effects on the 106 CCDs in the FPA from the analysis of the science data and dedicated calibration procedures. The paper shows first results and discusses the detected irradiation background with respect to predictions and reviews operational implications for the mission.

Keywords: Gaia, CCD, radiation, FPA, L2, CTI, PPE

1. INTRODUCTION

The Gaia satellite was successfully launched on December 19th 2013 from the European spaceport CSG (Centre Spatial Guyanais) near Kourou in French Guiana for its journey to the 1.5 million kilometers distant Sun-Earth Lagrange point 2 (L2). After launch and early orbit phase (LEOP) and a short transfer phase of one week duration the spacecraft was injected into its large Lissajous orbit around L2. The time of transfer was used to outgas the sensitive payload elements including mirrors and focal plane assembly (FPA).

The FPA with all 106 CCDs and proximity electronics modules (PEMs) was switched on for the first time on January 3rd 2014 during the initial phase of payload cooldown, which lasted more than 1.5 months to reach thermal equilibrium. FPA switch-on was followed by first spin up of the satellite on January 8th entering into a commissioning specific scan law over the ecliptic poles. Due to unforeseen problems, including an increased level of straylight [1], the originally planned 4 months of in-orbit commissioning have been extended and activities are still continuing before entering into the nominal scan law for the 5-year nominal duration of the mission.

While the focal plane detectors are already exposed for several months to the radiation environment at L2, the data analysis concerning radiation effects has been deferred due to the on-going commission activities and the presented results should therefore be seen as preliminary. All in-orbit procedures to assess the continuous effects of radiation damage have been successfully executed and will be repeated on a monthly to half-year cadence throughout the mission lifetime and a thorough analysis and trends will follow in due time. Most of the data collected during the commissioning phase will serve as zero point for the in-orbit performance evolution, but also comparisons to on-ground tests are done where appropriate.

*ralf.kohley@esa.int

High Energy, Optical, and Infrared Detectors for Astronomy VI, edited by Andrew D. Holland, James Beletic, Proc. of SPIE Vol. 9154, 915406 · © 2014 SPIE · CCC code: 0277-786X/14/$18 · doi: 10.1117/12.2056420

Before launch extended on-ground tests have been carried out to understand the effects of CTI on Gaia astrometry (line and point spread functions), spectro-photometry and spectroscopy (spectral mixing, charge loss, spectral resolution) caused by accumulated displacement damage from non-ionizing energy loss (NIEL) on the focal plane CCDs [2][3].

Models have been developed based on the on-ground test results that will be fed and optimized from the in-orbit data collected throughout the mission lifetime as radiation damage is constantly building up [4][5][6][7]. The data taken during commissioning will mainly serve to set the appropriate zero point for the radiation damage evolution.

2. RADIATION ENVIRONMENT, SHIELDING AND PREDICTIONS

Before launch Airbus Defense and Space (Airbus DS) carried out a detailed sector analysis to predict the accumulated ionizing dose and non-ionizing energy loss (NIEL) particle fluences on sensitive payload components taken into account the spacecraft and payload shielding. These end-of-life (EoL) dose and fluences entered the on-ground radiation tests as target values. The energetic particles the Gaia spacecraft is encountering on its journey to L2 and in its orbit around L2 are:

1) Trapped electrons and protons around the Earth

   The spacecraft has passed only for a few days through the radiation belts, which extend to some tens of thousands of kilometers from the Earth surface and the effect of these charged particles on the EoL radiation damage is therefore considered not significant. Also the Gaia focal plane was not switched on during this period and therefore any accumulated effects between ground and first FPA switch-on in orbit cannot be isolated as particular events. Radiation belt particles have been ignored in the sector analysis.

2) Galactic cosmic-ray (GCR) background

   These will be detected continuously during the mission, especially during solar "quiet" times. Due to the expected low flux level of GCRs, they will not significantly contribute to the EoL radiation damage, and were therefore also excluded from the sector analysis.

3) Solar energetic particles

   During the maximum solar activity period of the solar cycle, solar eruptions produce large fluxes of solar energetic particles, protons and heavy ions, which reach L2 when the eruptions are directed towards Earth. Heavy ions will not contribute significantly to the EoL radiation damage, and were therefore also excluded from the sector analysis, but may leave traces as strong transient events. The main contributor to transient events (detected cosmic ray traces) and accumulated EoL radiation damage will be solar protons. The expectation is that transient effects and radiation damage increase can be correlated to solar flare events.

2.1 Spacecraft and payload shielding

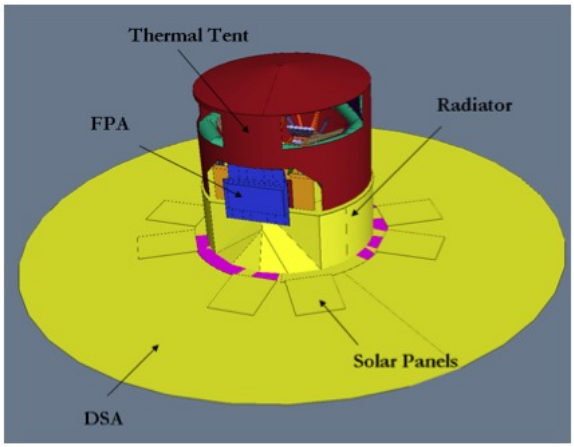

Figure 1: Main structural elements of the Gaia SVM and PLM modeling, whose material and geometrical shielding properties entered the sector analysis of radiation effects on the FPA. All SVM and PLM components not shown here were modeled in detail. Image courtesy of Airbus DS.

Apart from the radiation environment itself the spacecraft and payload shielding plays an important role in the assessment of radiation effects seen on the detector systems. Figure 1 gives an overview of shielding components that entered the on-ground sector analysis for the prediction of the End-of-Life (EoL) radiation dose and associated science performance prediction.

The FPA is shielded from below by the Service Module (SVM), which is housing the equipment boxes and propulsion system, and by the Deployable Sunshield Assembly (DSA) with the solar panels. The aluminum and CFRP thermal tent covers the Payload Module (PLM) comprising the SiC torus structure, the mirrors of the two TMA telescopes and support structures, fore optics for the photometer and radial velocity spectrometer instruments and the FPA itself.

Figure 2 gives a view to the elements surrounding the FPA CCDs in flight configuration. As can be seen from the sector analysis results (section 2.2), the photometer CCDs due to the shielding effect of the prisms and CCDs with location of restricted solid angle view due to vanes and side protection (SM, BAM and RVS) are the least affected.

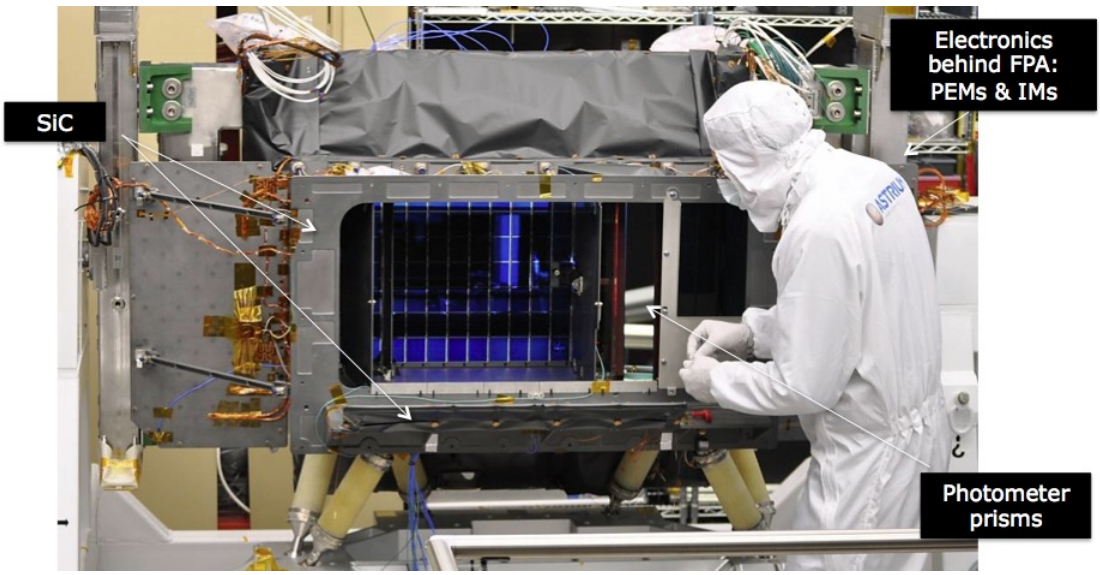

Figure 2: Assembled focal plane: the FPA is surrounded by the SiC cold radiator and individual FPA functional sections are divided by additional SiC vanes. From the front the photometer CCDs are protected by the prisms and all CCDs are protected from behind by the warm readout electronics. Image courtesy of Airbus DS.

2.2 Sector analysis

The predictions of end-of-life 10 MeV equivalent proton fluences and ionizing dose that entered the sector analysis are based on the JPL-1991 model for solar protons assuming as input a mission with 4 years of solar maximum activity period (representing an added margin).

The SHIELDOSE model has been used to derive the ionizing dose depth curve for Gaia and to derive the total ionizing dose for the individual components based on the absorbing properties of the shielding components.

Non-ionizing dose is evaluated through Non-Ionizing Energy Loss (NIEL) coefficients of particles in semi-conductors. By using the NIEL function normalized to 10MeV, one can derive the 10MeV equivalent proton damage fluence, which is presented in Figure 3.

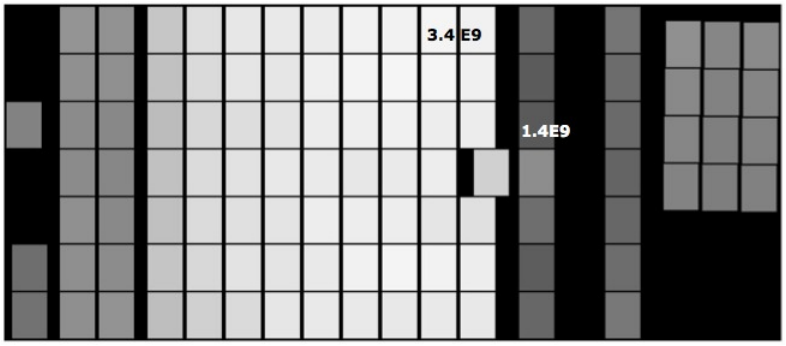

Figure 3: Sector analysis made by Airbus Defense and Space, France, of the expected proton irradiation ranging 3.4E9 p+/cm^2 in the astrometric field to 1.4E9 p+/cm^2 on the blue photometer CCDs. The mosaic configuration of the FPA is explained in Figure 5. Shielding is achieved by surrounding payload and spacecraft components, the FPA cold radiator and the installed vanes in between the different FPA parts. A clearly visible shielding effect is caused by the photometer prisms, which are installed on the cold radiator directly in front of the FPA.

2.3 Solar activity

Gaia was launched close to the maximum of solar activity during this solar cycle as shown in Figure 4 from the progression of the solar cycle sunspot numbers. In 2007 predictions were pointing to a solar maximum around beginning of 2012 and presented a large uncertainty in solar activity for the next cycle. Measurements confirm that this cycle doesn't follow anymore the regular 11-year period and while unfortunate for Gaia, the delay of the solar maximum by about 2 years, also exhibits less solar activity and expectations are that the end-of-life radiation dose and proton fluence will be less than predicted and assumed in the models.

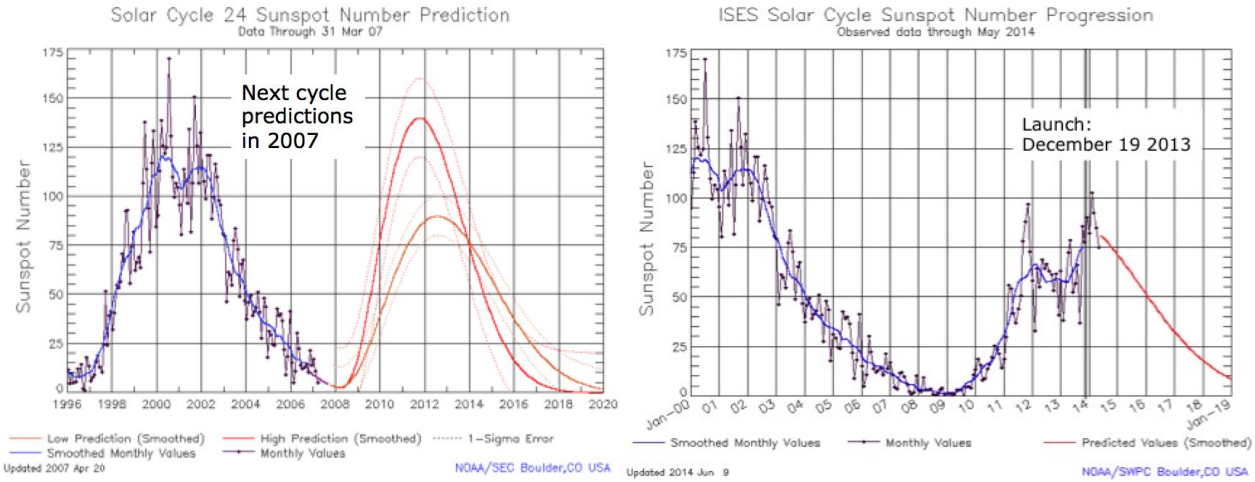

Figure 4: Solar activity predictions for current solar cycle in 2007 (left panel) and sunspot number progression until June 2014 (right panel) (NOAA/SWPC Boulder, CO USA).

3. FOCAL PLANE DESIGN AND OPERATION

The Gaia focal plane assembly and operations are detailed in [8] and an overview of the focal plane functions and CCD allocations is given in the schematics presented in Figure 5. All CCDs are operated in synchronous TDI readout mode with a TDI line time of 0.9828ms. The total integration time is therefore maximal 4.42s over the 4500 TDI stages, but can be reduced by activating one of the 12 special TDI gates that act as a barrier in the parallel charge transfer and therefore resets the TDI integration time in the extreme case down to about 2 ms. In the Sky Mapper (SM) CCDs a gate is permanently set to reduce the TDI integration time to 2.95s, which also reduces the effective area over which radiation effects including transients are being detected.

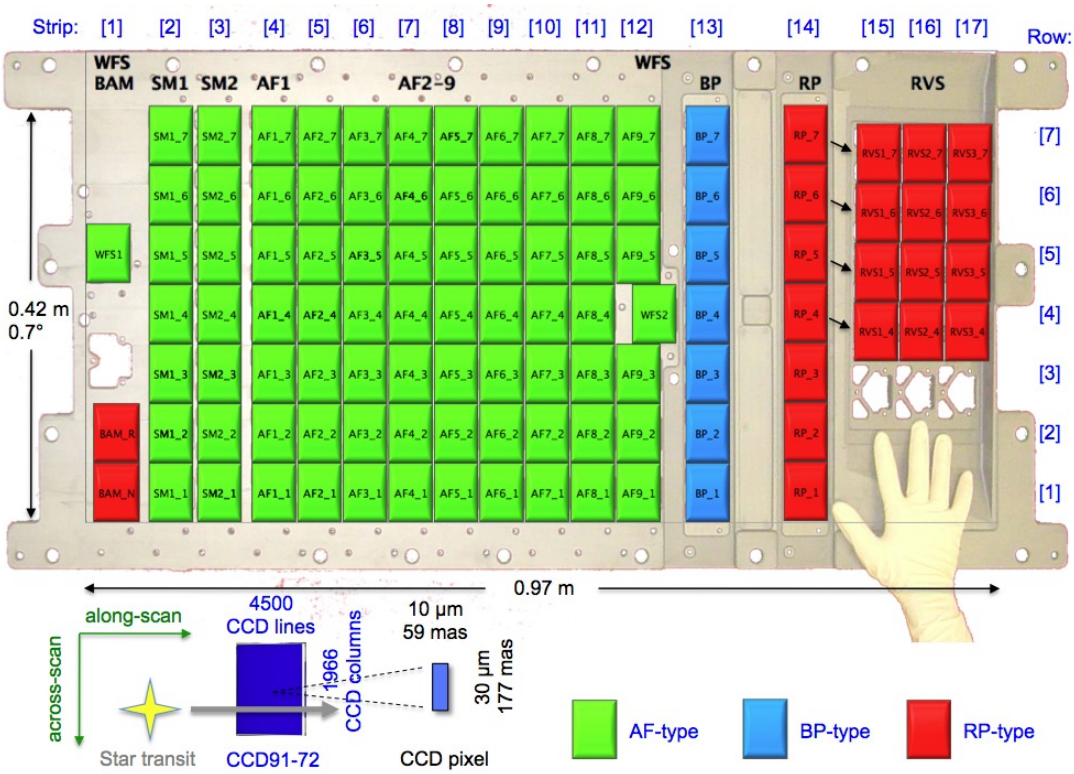

Figure 5: Part of the Gaia FPA with all 106 Flight Model CCDs mounted on the common SiC CCD Support Structure (CSS). The picture shows the view of the FPA after CCD integration and the 2 wavefront sensor optical assemblies placed as fore-optics in front of their respective CCDs. The e2v technologies CCD91-72 was manufactured in 3 variants: a broadband, standard silicon, 16µm thick AF-type, a blue-optimized, standard silicon, 16µm thick BP-type and a red-optimized, 40µm thick, deep-depleted RP-type. Most sensors are of the AF type including the 62 astrometric field (AF), 14 sky-mapper (SM) and the 2 wavefront sensor (WFS) CCDs. The blue photometer (BP) instrument consists of 7 BP type CCDs, which receive the dispersed light from the photometer prism mounted in front of the FPA. The red photometer (RP) instrument is analogous but using 7 RP type CCDs. Finally, the radial velocity spectrometer (RVS) instrument consists of 12 RP type CCDs in 3 × 4 arrangement receiving the narrow-band highly dispersed light from the RVS grating and optics mounted in the optical train on a support platform suspended directly from the torus. The schematic view below shows the mosaic arrangement of the focal plane in 7 rows and 17 strips and the assignment of the individual CCDs to the different instruments. Underlying image courtesy of Boostec Industries, France.

An exception are the CCDs for the Basic Angle Monitoring (BAM) device that can operate in stare mode to integrate the interference pattern produced by the on-board laser beams projected through both telescopes. These BAM CCDs integrate for 24 s before the TDI readout starts within each acquisition cycle. An example for the BAM acquisition is shown in Figure 13.

Most CCDs are read-out in windowing mode with windows assigned from the automatic object detection process, but additional predefined windows can be inserted into the acquisition stream to obtain information about charge injection signal and sky background, for example. SM CCDs are read out full frame with binning 2x2, but the full image is normally not downlinked due to downlink telemetry budget constraints.

The main characteristics of the Gaia e2v technologies CCD91-72's are as follows:

- 10µm x 30µm pixels
- 1966 columns x 4500 rows (TDI stages)
- 4 phase parallel register operated at 0.9828 ms TDI line time
- 2 phase serial register operated at 10 MHz clocking
- Single low noise amplifier

- Single drain-gate parallel charge injection structure and supplementary buried channel for radiation-induced CTI mitigation in along-scan direction
- Lateral anti-blooming drain
- 12 Special TDI gates to reset TDI integration
- Summing register for parallel binning
- Serial binning on output node
- 3 variants:
    - AF: 16µm, standard silicon, broadband AR
    - BP: 16µm, standard silicon, blue enhanced AR
    - RP: 40µm, deep-depleted, red enhanced AR

Considering radiation effects and their mitigation schemes three aspects are important: (1) the supplementary buried channel (SBC), which limits small signals to a smaller confinement volume, (2) the operation of charge injection, and (3) the different device variants, especially between the standard silicon AF type and the high-resistivity RP type.

The SBC and its impact on radiation induced CTI reduction has been analyzed in detail in [10], and is not repeated here. Charge injection is used as analysis and monitoring tool for different purposes and for systematic CTI mitigation: the charge injection point evolution is used to trace flatband voltage shifts (see section 5.1), first pixel response (FPR) and extended pixel edge response (EPER) are assessed from special user-defined readout windows placed over the charge injection lines and the charge release trails and regular charge injection is commanded for nominal mission (see section 5.2).

Lessons-learnt from Gaia CCD development and operations with respect to radiation damage effect mitigation have been transferred and implemented in the Euclid CCD design [11].

4. ON-GROUND TESTING

Prior to launch extensive tests on the assembled FPA and the individual CCD-PEM detector systems have been carried out. With respect to radiation damage assessment and procedures the most important have been the FPA and PLM thermal balance and thermal vacuum (TB/TV) in 2012 and from 2007 to 2013 five dedicated test campaigns on partially irradiated Gaia CCDs on a specially designed test bench facility, which allows projecting representative star images and spectra in TDI integration mode on the CCDs (see Figure 6). The implementation of the in-orbit procedures for radiation damage assessment and monitoring as tested during the PLM TB/TV tests were validated in Science Operations Validation Tests (SOVTs) in 2013.

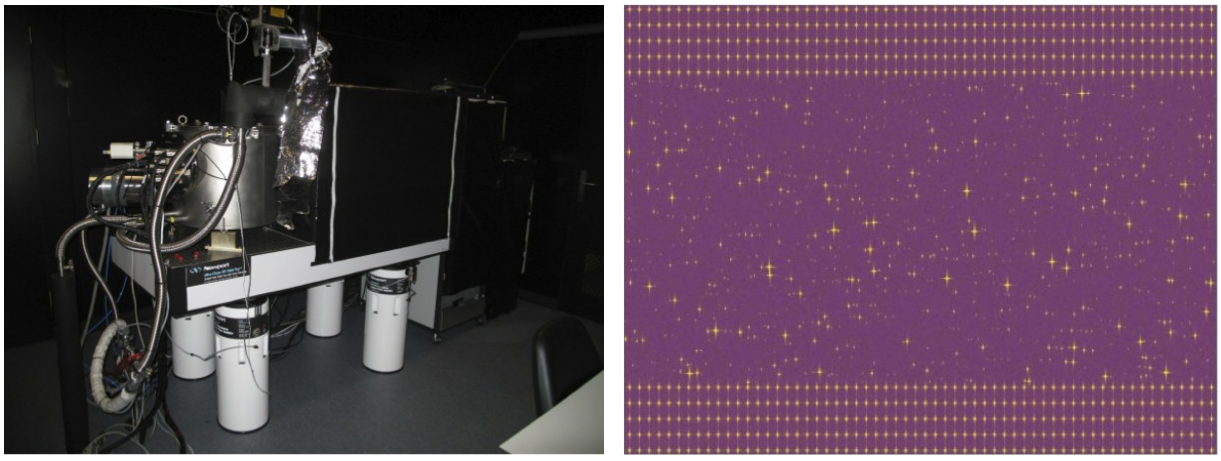

Figure 6: Left: Gaia test bench facility used for the on-ground radiation tests, now installed at ESTEC and used for CCD tests during operations. Image courtesy Peter Verhoeve. Right: Artists impression of “sky-like” mask for testing of radiation effects on astrometry. Image courtesy Denis Marchais.

During 2013 the test bench facility has been transferred to ESTEC to support Gaia operations and has been in use since then to assess on-ground the in-obit effects seen on the FPA CCDs [14]. The on-ground radiation tests have produced a wealth of information and had helped to develop the models implemented in the data processing chain to solve for the radiation induced CTI effects. The test results also allowed the trade-off for the operating temperature concerning serial and parallel CTI and to establish an optimum charge injection scheme for the astrometic field and photometer CCDs, implemented now as permanent mitigation and assessment means (see section 5.2).

The results from the PLM TB/TV tests are currently being cross-checked with the initial in-orbit results.

5. IN-ORBIT PROCEDURES, PREDICTIONS AND FIRST RESULTS

5.1 Ionizing damage

Ionizing damage on the CCDs mainly causes charge accumulation in the gate isolation oxides. This in turn causes an increase in flatband voltage shift, which can be measured on the Gaia CCDs as a shift in the charge injection turn-off point. The charge injection structure on the Gaia CCD91-72 is a simple injection drain and gate combination as depicted in Figure 7.

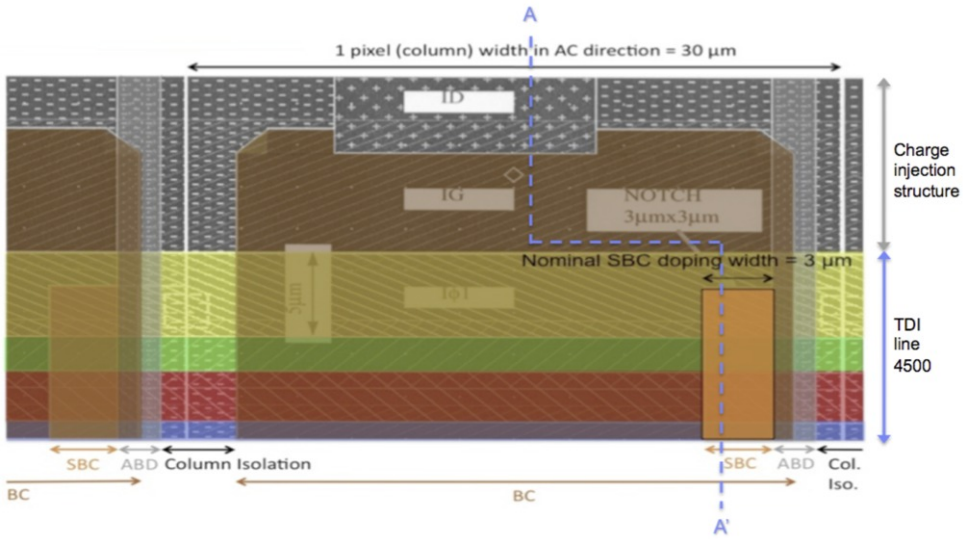

Figure 7: Photolithographic layers of Gaia CCD upper section (from [9], courtesy of G.M. Seabroke)

In the voltage-controlled method charge is injected into TDI line 4500 with the signal level being dependent on the difference between the potentials under the injection gate (IG) and the first image area phase Iϕ1. For the charge injection operation the injection drain voltage is clocked between the low rail (potential below injection gate potential = injection ON) and the high rail (potential above injection gate potential = injection OFF). For a fixed injection gate voltage (VIG) the injection drain low rail voltage can be successively increased until injection ceases, called the injection turn-off point. The time evolution of the turn-off voltage under unchanged operating conditions tracks the flatband voltage shift with ionizing dose.

The prediction for the Gaia CCDs is a total ionizing dose of 2krad(Si) EoL, resulting in a maximal flatband voltage shift of about 0.5V. The CCD operating point has been chosen to accommodate a flatband voltage shift of 0.5V without causing any degradation beyond the performances limits. Nevertheless, a constant long cadence tracking of the flatband voltage shift is required in-orbit to verify the predictions and to assess the need for counter-measures, if the trend would deviate from the expected EoL shift. The in-orbit procedure will therefore be repeated in regular intervals with approximately 6 months cadence.

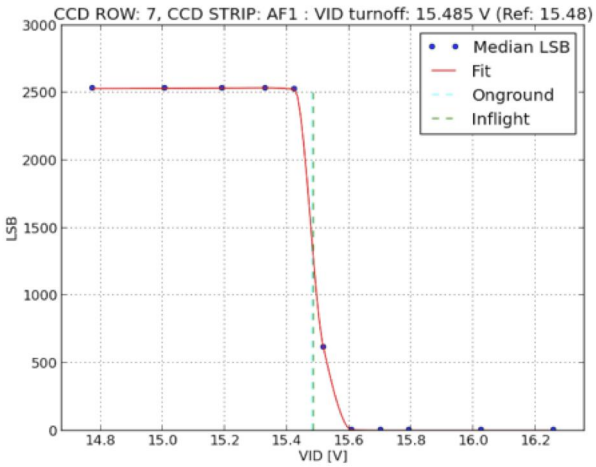

Figure 8: Under continuous charge injection conditions the injection drain voltage low rail is successively increased to assess the charge injection turn-off point (injected signal drops to zero). In this case the turn-off voltage has been determined to 15.485V as mid-point in the turn-off signature, which showed very good coincidence to the turn-off voltage measured on-ground (15.480V).

During commissioning two runs of the in-orbit procedure have been executed, an early run mid-January to validate the procedure and a second run beginning of April to set a in-orbit zero point for the tracking of the flatband voltage shift throughout the mission. Comparing the two in-orbit runs, it appears that the method is not precise enough to detect flatband voltage shifts below 0.1V. While this is not seen as critical, investigations have started to improve the precision of the method and to accurately track the associated shifts on the individual CCDs.

A comparison to the on-ground tests on the assembled FPA in the frame of the FPA and PLM TB/TV test campaigns has been carried out as well and is presented here in Figure 8 and Figure 9. The spread in measurements show the precision limit of the applied method, which should exhibit only positive deltas, e.g. an increase of VID low rail injection cut-off voltage with time under accumulated ionizing damage.

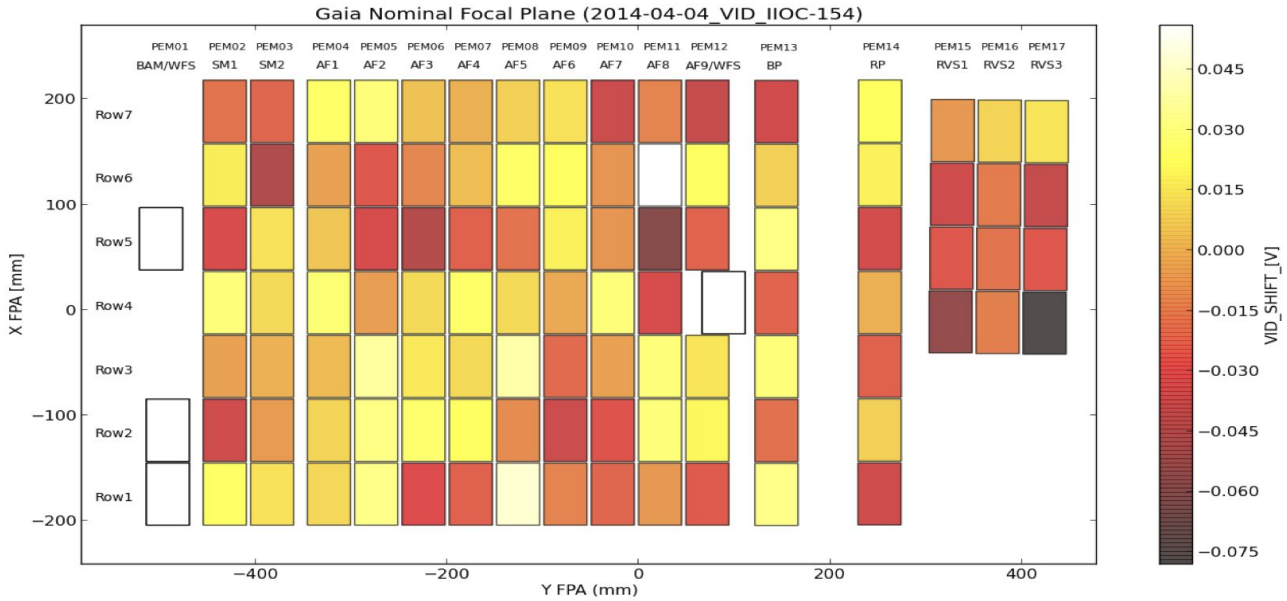

Figure 9: Flatband voltage shift assessment in focal plane context as delta to on-ground measurements. The voltage differences for the individual CCDs range from -0.08 to 0.05V, showing the precision limit of the method. True radiation induced flatband voltage shifts should all go to positive deltas.

The mean shift averaged over all individual CCD measurements in The FPA after 3 months at L2 compared to on-ground is: -0.002V ± 0.026V. Therefore, there are no indications for a global flatband voltage shift after this time in orbit within the measurement uncertainties, which coincides with the expectations.

5.2 Non-ionizing damage

Non-ionizing radiation on CCDs cause displacement damage of atoms in the silicon lattice creating new defect sites with energy levels within the silicon bandgap. Depending on the existing dopant atoms, different stable defect complexes are possible like the phosphorous-vacancy complex (or Si-E centre), di-vacancy (V-V) or oxygen-vacancy (Si-A centre). These defect locations if in the buried channel cause trapping sites that capture and defer electrons during the charge transfer process leading to charge loss and release trails. Trapping and de-trapping characteristics are highly temperature and clock timing dependent following Shockley-Read-Hall theory. Gaia CCDs have very different pixel shift times in parallel and serial directions and the Gaia CCD operating temperature of nominal 163K has been set to favour minimal radiation induced CTI in parallel or along scan over the serial or across scan direction without sacrificing negligible dark current.

The analysis of trap parameters and dependencies are subject to many studies, a few cited here especially in the Gaia and Euclid context [2][3][12][13]. From dedicated on-ground testing (section 4) models have been developed that are being implemented in the on-ground processing of the Gaia science data [5][6][7]. To bootstrap the models and to trace the radiation damage evolution over time, the CTI effects as exhibited through FPR and EPER measurements on injected charge lines are being analyzed. Figure 10 gives an example of a dedicated on-board procedure to assess radiation damage on SM CCDs. Serial as well as parallel CTI is being assessed.

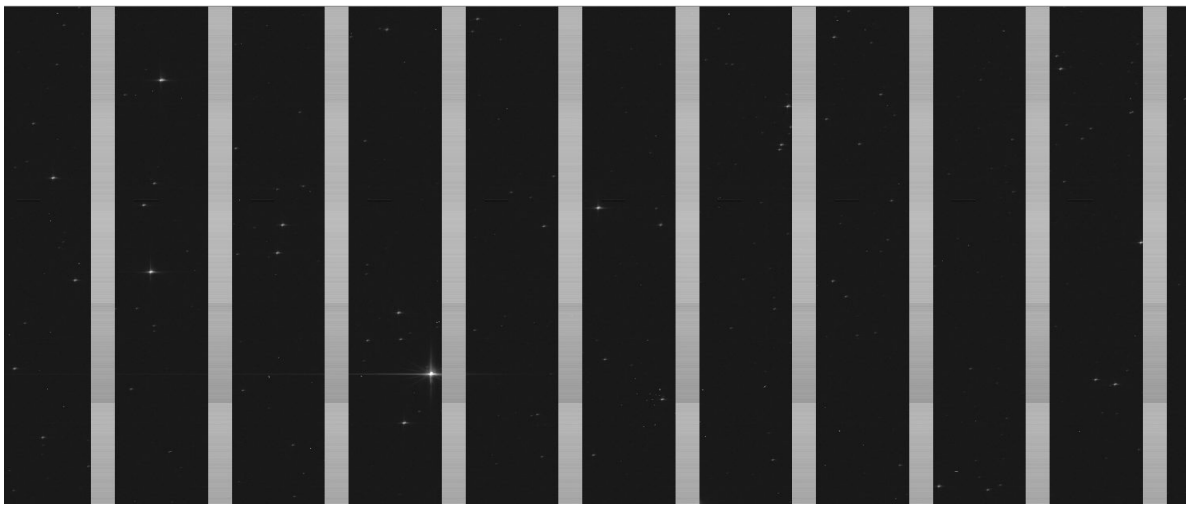

Figure 10: Blocks of injected charge lines to assess parallel and serial CTI. Gaia has no shutter for calibration observations, therefore all images are "polluted" by stars.

For parallel CTI, a regular charge injection scheme is in place that consists of:

- 4 lines of CI every ~2s (2000 TDI lines) at 18 ke- in AF field
- 4 lines of CI every ~5s (5000 TDI lines) at 19 ke- in BP/RP

The regular scheme has only been employed now, so data and analysis still outstanding. FPR and EPER will be measured from additional readout windows inserted into the stream of autonomously assigned object windows. EPER measurements are difficult to assess due to the faint de-trapping trail contaminated by the increased straylight background. For CCDs that do not employ the regular CI scheme specific in-orbit procedures have been set up.

For serial CTI, a specific in-orbit procedure acquires serial post-scan data together with readout window from the image area to assess the serial CTI trail for 5 different charge injection levels. Early in-orbit runs have been carried out to establish the serial CTI zero point. Due to the 2-phase register design, no serial FPR measurement possible. Figure 11 gives an example.

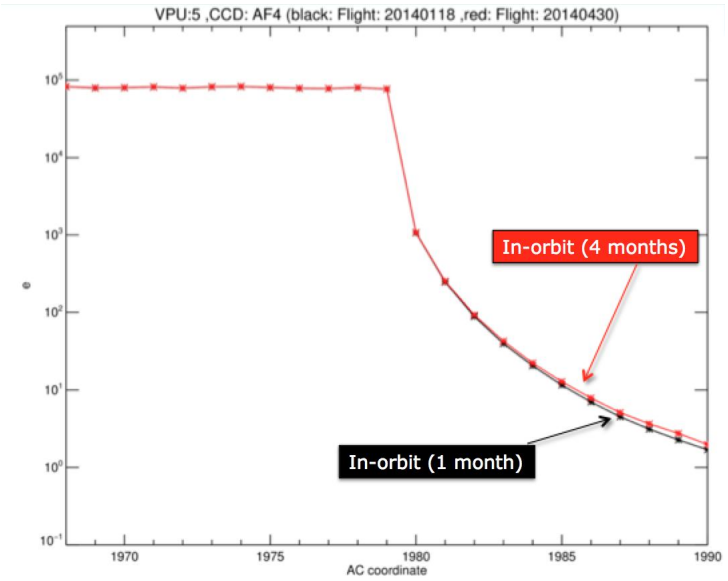

Figure 11: Example of charge trails analyzed from the serial CTI run after 1 month and after 4 months in-orbit. The increase in effective CTI is minimal between the two runs, which points to very few accumulated radiation damage during this time.

On-ground tests have shown that parallel CTI is worse on the RP variant compared to the AF/BP variant and for serial CTI the other way around. The in-orbit data collected so far did not show significant CTI evolution in-orbit. A more detailed analysis and comparison to on-ground data is still on going.

5.3 Transient events

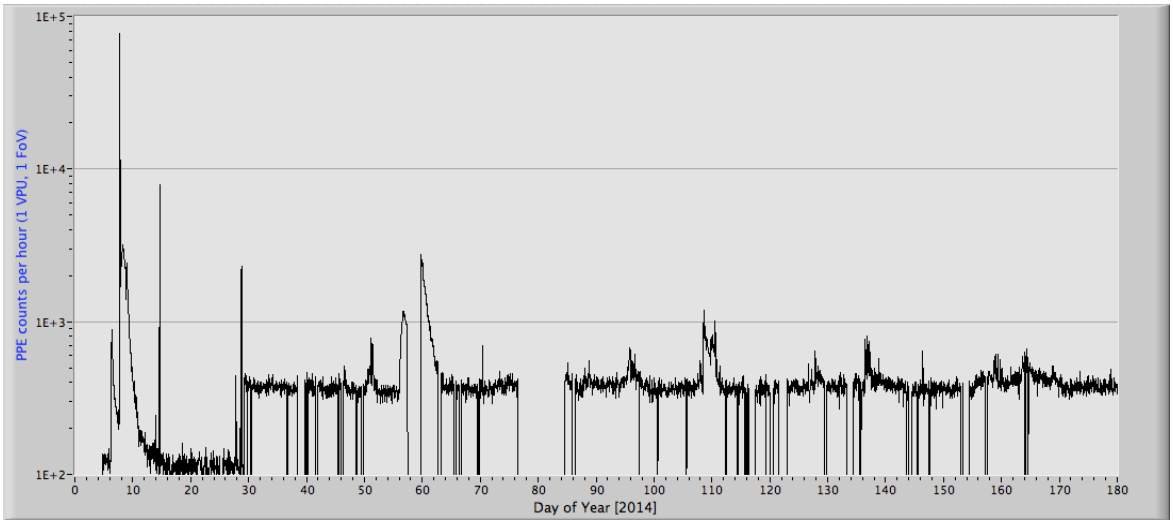

Figure 12: Example of the on-board PPE counter from the PPE filtering during the detection process. The spikes are correlated to solar activity like the intensive solar flare on the 7th of January 2014 (DoY 7). Interruptions and changes in the background count rate are due to changes to the spacecraft and payload configurations, which after commissioning should stabilize.

Transient events in form of prompt particle events (PPEs) leave different traces in the Gaia data. Two examples are presented here: (1) statistical counters based on the filtering mechanism in the on-board detection algorithms and (2) direct imaging of PPEs.

The first example of the on-board counters is a measurement of the overall PPE rate per detection area and signal threshold. The unbiased detection process on-board discriminates as a first filter PPEs from true objects with an integrated signal within the measurement window above a certain detection threshold based on morphology. As a second

step, if the detected object cannot be confirmed in the readout window of the next CCD strip, the object is discarded as PPE. On-board counters collect the number of rejected objects for each individual VPU row and field-of-view. The statistical evolution of all counters has been shown to follow the same trend and coincides in peak rates to solar activity events (solar flares). Figure 12 gives an example. The counters are reported through the housekeeping telemetry and can be easily retrieved.

The second method of direct imaging will allow estimation of deposited signal, cosmic ray track lengths, orientations and morphology, which cannot be retrieved from the counters themselves. The analysis is more complicated because no "dark" references frames are available due to the lack of an on-board shutter and only readout windows from limited areas on the CCDs are transmitted to ground. Binning modes, readout noise and gain change depending on which FPA function a certain CCD is assigned to. Analysis will be done at least on two types of CCDs, the standard AF variant and the deep-depleted RP variant. Figure 13 gives an "unusual" example, where the full CCD area was read out in a pseudo snapshot mode on a single RP variant CCD. Also the integration time for collecting events is in general very small with about 1ms per TDI line and 4.4s for the full CCD readout. A more detailed analysis is still pending.

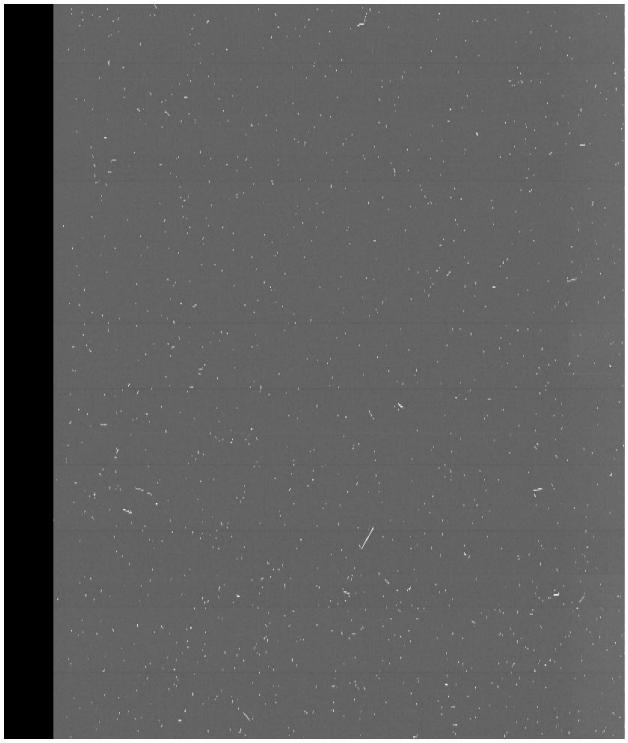

Figure 13: Example of cosmic rays impacts on a single RP CCD (BAM) read-out in a special readout scheme of time-shifted strips to cover the full detector width in samples binned 1x4. Due to the rectangular pixel size, these super-pixels are then 10x120µm2 in size. To better visualize the tracks, the image has been re-scaled to the physical extensions of the CCD. Readout is to the upper right corner with the single serial register in vertical direction.

6. CONCLUSIONS

Ionizing damage as manifested through flatband voltage shift has not been detected so far in-orbit within the measurement uncertainty. This corresponds to expectations and investigations have started to improve the measurement precision and possibly to extend the analysis to the output amplifier structure, if degradations are detected. In-orbit values will be taken as reference for mission lifetime.

Non-ionizing damage is being analyzed first concerning increase in serial CTI with data from EPER of deferred charge into the serial postscan. Serial FPR measurements are not possible on Gaia CCDs. Data is already available from two in-orbit runs, one shortly after FPA switch-on and another run three months later. The increase in serial CTI deferred charge trails is minimal between the two runs, and differences to on-ground tests are being attributed to in-orbit FPA CCD temperature and distribution under nominal operational conditions being (slightly) different from ground testing. Parallel

CTI analysis is still pending due to the regular charge injection scheme being activated at the end of the performance verification phase. Like for the ionizing damage assessment, the in-orbit values will be taken as reference for mission lifetime. Most data concerning the evolution of trap population will come from nominal processing of star images themselves and CTI effects being solved for in the data processing.

Transient effects in terms of cosmic ray interactions are detected on all CCDs at all times, but under different readout configurations. The on-board detection process is filtering false detections triggered by prompt particle events and storing this information in on-board counters reported in housekeeping telemetry. These counters give a first indication of the PPEs background at L2 and correlation to solar activity. A more detailed analysis of deposited charge, track lengths and morphology will follow in due time. This analysis suffers from the difficulty of not having "Dark" reference images available due to the lack of an on-board shutter.

All in-orbit radiation monitoring procedures have been validated and provide zero points for damage evolution for the rest of the mission. These dedicated procedures will be inserted as calibration activities with 1 to 6 months cadence to monitor evolution at regular intervals apart from the continuous information embedded in the science and housekeeping telemetry.

The focal plane has been switched on the 3rd of January 2014 and all 106 CCDs and PEMs have been working flawlessly so far delivering excellent performance and calibration stability in-orbit.

ACKNOWLEDGEMENTS

Material used in this work has been provided by Gaia MOC teams and the Coordination Unit 1 (CU1) of the Gaia Data Processing and Analysis Consortium (DPAC). It is gratefully acknowledged for their contribution.

REFERENCES

[1] Prusti, T., "Gaia: scientific in-orbit performance", Proc. SPIE 9143, this conference (2014).
[2] Hopkinson, G.R., et. al., "Radiation effects on astrometric CCDs at low operating temperatures", IEEE Transactions on Nuclear Science, Vol. 52, no. 6, (2005).
[3] Hopkinson, G.R., Garé, P. Sarri, G., "Effects of Low Temperature Proton Irradiation on a Large Area CCD for Astrometric Applications", IEEE Transactions on Nuclear Science, Vol. 57, no. 4, (2010).
[4] Seabroke, G.M., et. al., "Modelling radiation damage to ESA's Gaia satellite CCDs", Proc. SPIE 7021, (2008).
[5] Prod'homme, T., et. al., "Electrode level Monte Carlo model of radiation damage effects on astronomical CCDs", MNRAS, Vol. 414, (2011).
[6] Short, A., et. al., "A fast model of radiation-induced electron trapping in CCDs for implementation in the Gaia data processing", Proc. SPIE 7742, (2010).
[7] Prod'homme, T., et. al., "Comparison of a fast analytical model of radiation damage effects in CCDs with experimental tests", Proc. SPIE 7742, (2010).
[8] Kohley, R., et. al., "Gaia's FPA: sampling the sky in silicon", Proc. SPIE 8442 (2012).
[9] Seabroke, G.M., "Silvaco ATLAS model of ESA's Gaia satellite e2v CCD91-72 pixels", Proc. SPIE 7742 (2010).
[10] Seabroke, G.M., et. al., "Digging supplementary buried channels: investigating the notch architecture within the CCD pixels on ESA's Gaia satellite", MNRAS, Vol. 430, Issue 4, p.3155-3170, (2013).
[11] Short, A.D, et. al., "The Euclid VIS CCD detector design, development, and programme status", Proc. SPIE 9154, this conference (2014).
[12] Hall, D.J, et. al., "In situ trap parameter studies in CCDs for space applications", Proc. SPIE 9154, this conference (2014).
[13] Prod'homme, T., et. al., "A comparative study of charge transfer inefficiency value and trap parameter determination techniques making use of an irradiated ESA-Euclid prototype CCD", Proc. SPIE 9154, this conference (2014).
[14] Verhoeve, P., et. al., "CCD characterisation for space missions at ESA", Proc. SPIE 9154, this conference (2014).